Available online at www.sciencedirect.com
ScienceDirect
Electrochimica Acta 53 (2008) 2115–2120
ELECTROCHIMICA Acta
www.elsevier.com/locate/electacta

Overpotential deposition of copper on an iodine-modified Au(1 1 1) electrode

Alejandro Martínez-Ruíz [a,*], Manuel Palomar-Pardavé [b], Nikola Batina [c]

[a] *Facultad de Ciencias, Universidad Autónoma de Baja California, Ensenada, BC 22800, Mexico*
[b] *Departamento de Materiales, Universidad Autónoma Metropolitana-Azcapotzalco, C.P. 02000 México, D.F., Mexico*
[c] *Departamento de Química, Universidad Autónoma Metropolitana-Iztapalapa, 09340 México, D.F., Mexico*

Received 23 June 2007; received in revised form 3 September 2007; accepted 4 September 2007
Available online 8 September 2007

Abstract

Cyclic voltammetry, chronoamperometry and in situ electrochemical scanning tunneling microscopy were used to study the kinetics of nucleation and crystal growth during the initial stages of copper overpotential deposition (OPD) on a previously iodine-modified Au(1 1 1) electrode, from an aqueous solution 10^{-3} M $CuSO_4$ in 0.05 M H_2SO_4. The starting potential during step experiments was chosen in the region where the gold electrode was completely free of the copper deposit. The recorded current transients for copper deposition onto the iodine-modified Au(1 1 1) electrode surface appear to be very complex, with the unusual presence of two or more current maxima. A new method was used for quantitative evaluation of current transients that involves the transition UPD–OPD, developed by our group [M. Palomar-Pardavé, I. González, N. Batina, J. Phys. Chem. B 104 (2000) 3545], was used for the quantitative interpretation. Our results show that, within a single current transient, copper adsorption and two types of nucleation process: two-dimensional (2D) and three-dimensional (3D) limited by lattice incorporation of copper adatoms and diffusion of Cu(II) ion, respectively, take place simultaneously. STM images revealed the enhanced growth of 3D copper on edge of I–Au(1 1 1) during the early stages of deposition. Moreover, our results strongly suggest that the iodine adlayer is constantly present, even after the striping Cu that was overpotential deposited.

Keywords: Copper; Overpotential deposition; Electrochemical STM; Electrocrystallization

1. Introduction

Nowadays, bulk Cu deposition is a technologically highly relevant process with work directed toward characterizing and controlling the texture and development of the deposit. A detailed understanding of the mechanism of growth of bulk electrochemical deposits remains to be elucidated, in part because of the complexity of the process and in part because the tools necessary for understanding these are only now being developed. Work in the area of bulk deposition using surface techniques as electrochemical scanning tunneling microscopy (ECSTM) and electrochemical methods as cyclic voltammetry (CV) and chronoamperometry (CA) is divided into research addressing the initial phases of bulk deposition, the subsequent growth of the deposit, and the influence of specific electrolytes or modified surface electrode on texture and growth. Considerable effort has put especially on the deposition of Cu because it deposits at a potential positive to that of hydrogen evolution.

Kolb and co-workers [1,2] showed that in the absence of additives, deposition of Cu occurs first at edges, dislocations, and defects in the Au(1 1 1) substrate surface, followed by deposition on terraces at longer times. However Cu electrodeposition process can be influenced by several parameters: the applied electrode potential (UPD or OPD), deposit's growth (2D or 3D) kinetics and mechanism, electroactive species concentration and deposit–substrate interaction [3–10]. Since UPD and OPD take place at more positive or negative, respectively, potentials than the corresponding Nernst equilibrium value, thus in several cases the OPD process takes place on an electrode surface that has already been modified by the UPD adlayer, rather than on the bare electrode substrate. Therefore in this case, UPD may involve Cu deposition onto Au(1 1 1) substrate while OPD would

* Corresponding author. Tel.: +52 646 1 74 45 60; fax: +52 646 1 74 45 60.
E-mail address: alejandro@uabc.mx (A. Martínez-Ruíz).

0013-4686/$ – see front matter © 2007 Elsevier Ltd. All rights reserved.
doi:10.1016/j.electacta.2007.09.011

involve Cu deposition onto a Au(1 1 1) surface modified by a Cu monolayer, which was formed during the UPD process. Höltzle et al. [11,12] and Palomar-Pardavé et al. [8] studied the kinetics of Cu UPD and OPD, respectively, onto a bare Au(1 1 1) surface or modified by a Cu UPD adlayer [8]. Recently [10] our research group showed the influences of a previously deposited iodine adlayer on the Au(1 1 1) surfaces onto the copper UPD kinetics, notwithstanding the effect of this kind of adlayer on Cu OPD has not been studied yet.

The halogens have been especially well studied in ultra-high vacuum (UHV) systems and are usually easily imaged in STM electrochemical environment. Iodine exhibits the strongest adsorption to many metals in electrochemical systems. The strength of the metal–iodine interaction has led to its use as a passivating layer to protect surfaces after flame annealing for transfer throughout the atmosphere. Tao and Lindsay [13] found that iodine on Au(1 1 1) exhibited a $(\sqrt{3} \times \sqrt{3})R30^\circ$ structure at low potentials, and close packed (3×3) structure at higher potentials. A similar situation is observed by Yamada et al. [14], Batina et al. [15] and Martinez-Ruiz et al. [9], at low potentials, the latter authors reported a rectangular $c(p \times \sqrt{3}R - 30^\circ)$ overlayer which compress from $p = 3$ to 2.49 as the potential is raised.

Therefore, in this work we will determine, using CV, CA and ECSTM, the influence of a pre-adsorbed iodine layer onto Au(1 1 1) on the Cu OPD process and we will show the usefulness of a recently developed method [8], which is capable of handling and interpreting complexly shaped experimental current density transients also taking into account different individual contributions involved during Cu OPD.

2. Experimental

Cyclic voltammetry (CV) and chronoamperometry (CA) as well as in situ electrochemical scanning tunneling microscopy (ECSTM) were employed to study the copper OPD electrocrystallization mechanism on iodine-modified Au(1 1 1) substrate from an electrolytic bath containing 10^{-3} M $CuSO_4$ in 0.05 M H_2SO_4 (pH 1). This electrolytic solution was carefully deaerated for 30 min using high-purity nitrogen gas. The chemicals used were suprapure grade from Merck. All solutions were prepared with ultrapure water (Millipore Milli-Q^{TM}).

All the electrochemical experiments were carried out in a conventional three-electrode cell system using an Au(1 1 1) or I–Au(1 1 1) working electrode, a platinum wire counter electrode and copper wire as reference electrode. The Au(1 1 1) was a 200 nm-thick gold layer evaporated onto "Robax" glass (AF. Berliner Glass KG. Germany), with 2 nm-thick chromium undercoating for better adhesion to the glass surface. To prepare an I–Au(1 1 1) electrode surface, this Au(1 1 1) film was annealed in a hydrogen flame for 1 min, cooled in hydrogen atmosphere, and then immersed in 1 mM KI aqueous solution for 3 min. Then the sample was thoroughly rinsed with pure 0.05 M H_2SO_4 and quickly transferred into the electrochemical cell.

For the experimental techniques CV and CA we used a PAR 289 (EG&G) potentiostat, or a BAS 100B (BioAnalyticalsystems) potentiostat, both coupled to personal computer. A STM (Nanoscope III, Digital Instruments, USA) was used for imaging of the I–Au(1 1 1) surface electrode.

The results of chronoamperometric measurements of the kinetics and mechanism of copper electrocrystallization onto I–Au(1 1 1) electrode surface were quantitatively evaluated using a homemade software package developed for the PC computer system. The set of potentiostatic current density transients (j–t curves) obtained was analyzed to estimate how many contributions and which mechanisms are involved in the electrocrystallization process. The next step was to plot the experimental data obtained in non-dimensional plots to determine the mechanisms involved with more accuracy. Major kinetic parameters for each process involved in the deposition reaction, as well as the relationship between different mechanisms were obtained from theoretical transients.

3. Results and discussion

3.1. Cyclic voltammetry

Cyclic voltammetry was used to define a potential region where the initial stages of copper overpotential deposition on iodine-modified Au(1 1 1) electrode occurs. Copper was deposited onto I–Au(1 1 1) substrate from an electrolytic bath containing 10^{-3} M $CuSO_4$ in 0.05 M H_2SO_4. Voltammetric scan were performed in several potential ranges between 0.350 V and −0.400 V vs. Cu/Cu^{2+} reference electrode. The sweep potential was always initiated at 0.350 V toward the negative direction.

Fig. 1 shows a voltammogram where the potential is within the −0.150 V and 0.350 V range, recorded at the scan rate

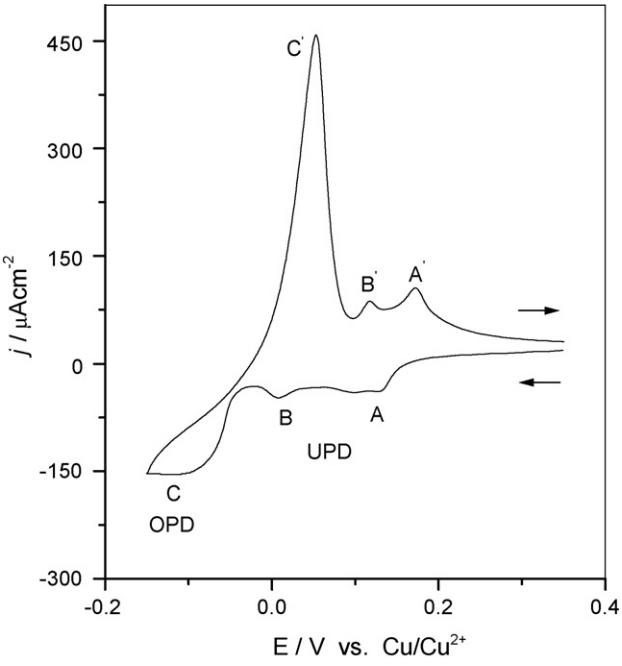

Fig. 1. Cyclic voltammogram for copper deposition onto I–Au(1 1 1) from 1 mM $CuSO_4$ + 0.05 mM H_2SO_4. The potential scan starts at 0.350 V, with a scanning rate of 15 mV s^{-1}. The voltammogram shows the copper UPD ($E > 0.00$ V, peaks A, B) and OPD ($E < 0.00$ V, peak C) deposition regions.

of 15 mV s^{-1}. In this voltammogram we can observe characteristic voltammetric peaks associated with Cu UPD onto I–Au(1 1 1) electrode: $A = 0.126$ V, $B = 0.008$ V and their corresponding oxidation peaks: $A' = 0.172$ V, $B' = 0.117$ V [9,10]. Peaks $C = -0.098$ V and $C' = 0.053$ V correspond to Cu OPD and dissolution process onto I–Au(1 1 1) electrode, respectively. In this voltammogram one can notice both types of copper deposition: UPD and OPD. More details concerning the cyclic voltammogram for UPD of copper onto I–Au(1 1 1) from bath containing 10^{-3} M $CuSO_4$ in 0.05 M H_2SO_4 can be found elsewhere [9,10].

Fig. 2 depicts an experimental cyclic voltammogram, varying the applied potentials within the Cu UPD region, recorded in the system: I–Au(1 1 1)/10^{-3} M $CuSO_4$, 0.05 M H_2SO_4 after applying several OPD cycles in the region of −0.4 V and 0.350 V. It is very important to note that the typical Cu voltammogram was obtained in the UPD region onto I–Au(1 1 1) [9,10]. This result strongly suggests that the iodine adlayer remains on the gold surface, even after the striping of Cu that was overpotential deposited.

3.2. Chronoamperometry

Applying potential steps allowed the acquisition of current density transients. Fig. 3 shows a set of experimental current density transients. All of them recorded at potential values around

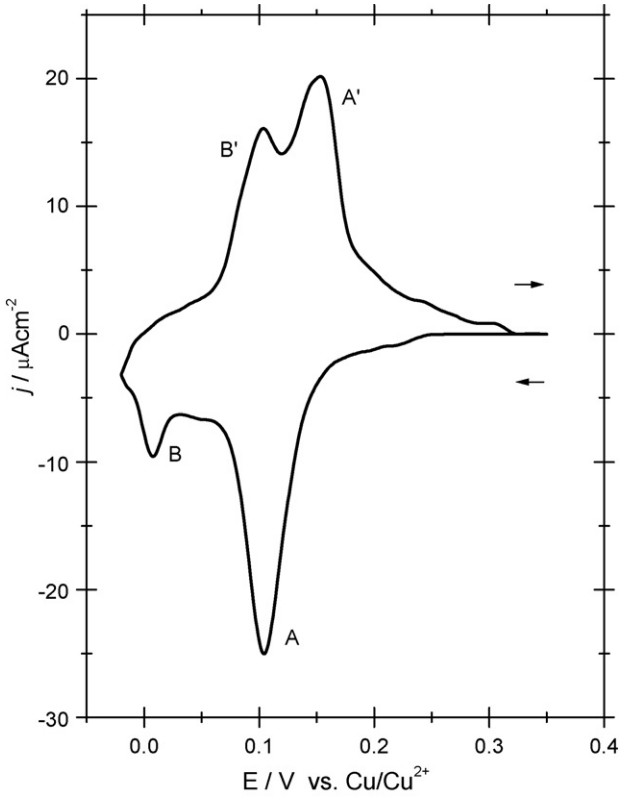

Fig. 2. Cyclic voltammogram for Cu UPD on I–Au(1 1 1) in electrolytic bath containing 1 mM $CuSO_4$ in 0.05 M H_2SO_4, scan rate of 15 mV s^{-1}, starting at 0.350 V electrode potential. This voltammogram was recorded after several cycles like that shown in Fig. 1.

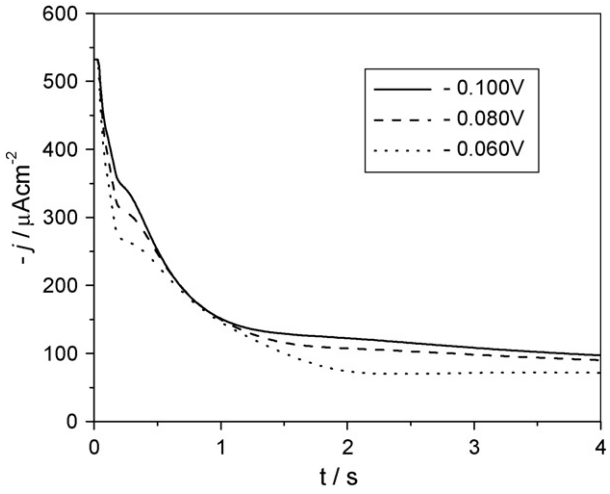

Fig. 3. Set of experimental current density transients recorded for copper OPD onto I–Au(1 1 1) surface from 1 mM $CuSO_4$ in 0.05 M H_2SO_4, solution, at different electrode potential (−0.06 V, −0.08 V and −0.10 V). In all cases the starting potential was 0.350 V.

peak C, see Fig. 1, which correspond to the Cu OPD region on the I–Au(1 1 1) substrate. All current transients present an initial decay due most likely to Cu(II) ions adsorption stage (i.e. charging of an adsorption pseudo-capacitance) as was proposed by Mendoza-Huizar et al. for cobalt UPD [16] and the transition UPD–OPD [14] onto a gold electrode. This falling current is followed by a not well-defined current maximum. This maximum shifts to shorter times when the potential step (or final cathodic potential) increases. The general shape of these transients, which is independent of the final potential, indicates the presence of a nucleation and growth process [7,8,16–21]. In order to determine the mechanism of nucleation and growth of the Cu OPD process on iodine-modified Au(1 1 1), we also analyzed the experimental data by performing usual procedures. According to the Cottrell equation (1), the plot j vs. $t^{-1/2}$ of diffusion-controlled process should be a straight line. Fig. 4 shows the plot j vs. $t^{-1/2}$ of the experimental transient recorded at −0.1 V, see Fig. 3, corre-

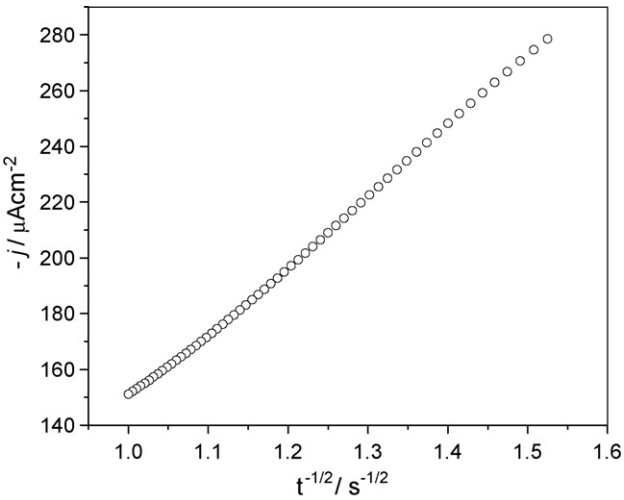

Fig. 4. j vs. $t^{-1/2}$ plot corresponding to indicating the current density transient recorded at −0.10 V, see Fig. 3.

sponding to the higher values of time. This plot can be adjusted by means of line regression giving 246.3 μA $s^{1/2}$ as slope, of 12.44 μA as intercept and a linear regression coefficient of 0.999. This behavior indicates that Cu nucleation process onto iodine-modified Au(1 1 1) electrode, at least for the final part of the transient, was a diffusion-controlled process. Using the slope value and Eq. (1) we obtained a value for the Cu^{2+} diffusion coefficient, D, of 8.51×10^{-6} cm^2 s^{-1} which is very similar to $D = 7.8 \times 10^{-6}$ cm^2 s^{-1} from the literature [8,12].

$$j = nFCD^{1/2}\pi^{-1/2}t^{-1/2} \tag{1}$$

Quantitative interpretation of these current transients was performed according to the Palomar-Pardavé et al. model [8] using the following equation:

$$j(t) = j_{\mathrm{Ad}}(t) + j_{\mathrm{2Di\text{-}Li}}(t) + j_{\mathrm{3D\text{-}DC}}(t) \tag{2}$$

where $j_{\mathrm{Ad}}(t)$ is the current transient due to Cu(II) ions adsorption stage (i.e. charging of an adsorption pseudo-capacitance), $j_{\mathrm{2Di\text{-}Li}}(t)$ is the current contribution due to 2D instantaneous nucleation followed by the lattice incorporation process, and $j_{\mathrm{3D\text{-}DC}}(t)$ is the current due to a 3D nucleation process followed by a diffusion-controlled growth. A quantitative estimate of the Cu(II) ions adsorption contribution was based on Langmuir-type adsorption–desorption equilibrium and the mathematical formalism previously used by Kolb and co-workers [6] is represented by the following equation:

$$j_{\mathrm{Ad}}(t) = k_1 \exp(-k_2 t) \tag{3}$$

where $k_1 = k_2 q_{\mathrm{ads}}$, and k_1 is related to the total charge due to the adsorption process (q_{ads}).

To describe the 2D instantaneous nucleation, the model developed by Bewick, Fleishmann and Thirsk (BFT) [22] was used. The BFT model was developed to describe a 2D growth, determined by the lattice incorporation of adatoms to the periphery of the growing nuclei. The BFT model is given by the following equation:

$$j_{\mathrm{2Di\text{-}Li}}(t) = \frac{2\pi z F M h N_0 K_g^2 t}{\rho} \exp\left(-\frac{\pi M^2 N_0 K_g^2 t^2}{\rho^2}\right) \tag{4}$$

Eq. (4) describes the current transient due to an instantaneous two-dimensional nucleation process, where K_g is the lateral growth rate constant of nuclei, h the height of the deposited layer, zF the molar charge transferred during electrodeposition, N_0 the number density of active sites, t the time, and M and ρ are the atomic weight and the density of the deposit, respectively.To describe the three-dimensional diffusion-control process, we used the model proposed by Scharifker et al. [18]:

$$j_{\mathrm{3D\text{-}DC}}(t) = \left(\frac{zFD^{1/2}C^{\infty}}{\pi^{1/2}t^{1/2}}\right) \times \left(1 - \exp\left\{-N_0\pi k' D\left[t - \frac{(1-\exp(-At))}{A}\right]\right\}\right) \tag{5}$$

where

$$k' = \frac{4}{3}\left(\frac{8\pi C^{\infty} M}{\rho}\right)^{1/2} \tag{6}$$

A parameterized form of Eq. (2) can be written as

$$j(t) = k_1 \exp(-k_2 t) + P_1 t \exp(-P_2 t^2) + P_3 t^{-1/2}(1 - \exp(-P_4\left(t - \frac{(1-\exp(-At))}{A}\right) \tag{7}$$

where $P_1 = (2\pi z F M h N_0 K_g^2/\rho)$, $P_2 = (\pi M^2 N_0 K_g^2/\rho^2)$, $P_3 = (zFD^{1/2}C^{\infty}/\pi^{1/2})$, and $P_4 = N_0\pi k' D$.

Calculation of theoretical current transients involves nonlinear fitting of Eq. (7) to experimental transient, via simultaneous variation of all parameters, according to the Marquadt–Levenver algorithm [21].

Fig. 5 shows the best fit, for the situations between experimental transients and theoretical counterparts considering Ad, 2Di-Li and 3D-DC processes. There is a very good agreement between the experimental results and the addition of the three theoretical components. The OPD process leads to overlapping between 2D and 3D nucleation, and the UPD maximum disappears. Table 1 shows the parameter values of the theoretical transients used to fit the experimental current transients presented in Fig. 5.

The nonlinear fitting of Eq. (7) performed on the current–time curves is shown in Fig. 5, with good agreement between our experimental results and the proposed model. The partial contributions, $j_{\mathrm{2Di\text{-}Li}}$ and $j_{\mathrm{3D\text{-}DC}}$ are assigned to the copper UPD and to the copper OPD, respectively. These results demonstrate that formation of 2D UPD copper film occurs simultaneously with the OPD. The total charge distribution between copper UPD and OPD process (Table 1) is also interesting to analyze. The total charge, see Q_{total} (exp) in Table 1, of each single transient was estimated from integration of the experimental curve. Partial charge contributions for Ad, q_{Ad} (theor), and 2D-Li process, $q_{\mathrm{2Di\text{-}Li}}$ (theor), both of which should be attributed to the UPD process, were estimated from integration of the theoretical curves while the charge related to the 3D-DC process (copper OPD), $q_{\mathrm{3D\text{-}DC}}$ (theor), was calculated as the difference between total charge and UPD contribution. For the UPD process, the charge involved varied from 232 mC cm^{-2} to 372 mC cm^{-2}, which is lower than 390 mC cm^{-2} corresponding to the formation of a pseudomorphic copper monolayer on the Au(1 1 1) surface [8,9]. From Fig. 5 it is possible to note that Cu OPD process started before the surface was covered by copper UPD (Ad + 2D-Li) which may explain why the expected charge density value for full monolayer coverage, 390 mC cm^{-2}, was not reached under our experimental conditions.

It is interesting to compare values of the kinetic parameters for copper growth in OPD in experiments carried out onto iodine-free Au(1 1 1) [8] and copper onto iodine-modified Au(1 1 1) surface (Table 1). The copper OPD nucleation rate (A) on the iodine-modified Au(1 1 1) surface is significantly higher than that for copper OPD onto bare Au(1 1 1), see Table 2 in Ref. [8]. The copper OPD nucleation rate (A) on the iodine-modified Au(1 1 1) surface increase as the overpotential increased while

Table 1
Kinetic parameters obtained from the nonlinear fitting of Eq. (7) to the potentiostatic current transients

E (V)	$Q_{total(exp)}$ ($\mu C\,cm^{-2}$)[a]	j_{Ad}			$j_{2Di\text{-}Li}$		$j_{3D\text{-}DC}$				
		k_2 (s^{-1})	k_1 ($\mu A\,cm^{-2}$)	$q_{Ad(theor)}$ ($\mu C\,cm^{-2}$)[b]	N_0 ($kg^2/mol^2\,cm^{-6}\,s^{-2}$)	$q_{2Di\text{-}Li(theor)}$ ($\mu C\,cm^{-2}$)[b]	D ($\times 10^6\,cm^2\,s^{-1}$)	A (s^{-1})	N_0 ($\times 10^{-6}\,cm^2$)	AN_0 ($\times 10^{-6}\,cm^{-2}\,s^{-1}$)	$q_{3D\text{-}DC(theor)}$ ($\mu C\,cm^{-2}$)[b]
0.05	698	1.40	480	342	0.0008	130	8.51	0.1	0.60	0.06	226
0.08	1049	5.86	1317	225	0.0076	103	8.51	0.42	2.12	0.89	721
0.10	1189	6.61	1317	199	0.0167	125	8.51	0.65	4.83	3.14	865
0.15	1275	8.26	1317	159	0.0167	124	8.16	0.75	4.83	3.62	992
0.20	1410	7.86	900	114	0.0499	118	8.15	1.35	5.66	7.64	1178

[a] Calculated from integration of the experimental transient.
[b] Calculated from the theoretical contribution.

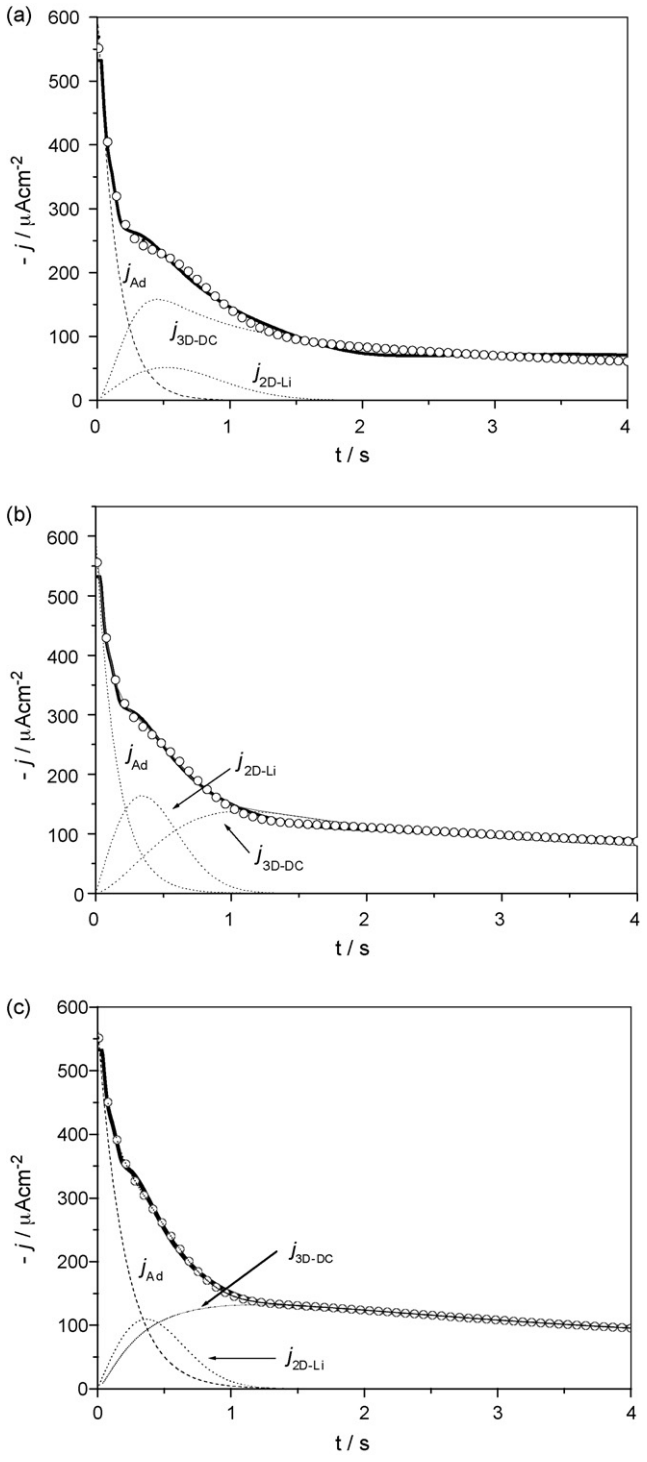

Fig. 5. Comparison between an experimental current density transient (O), recorded during copper OPD on I-modified Au(1 1 1) when a potential value of (a) −0.06, (b) −0.08 and (c) −0.10 V was applied (see Fig. 3) with a theoretical transient (—) generated by nonlinear fit of Eq. (5) to the experimental data. This figure depicts the different individual contributions comprising Eq. (5).

the nucleation rate for copper OPD onto Au(1 1 1) decreased as the overpotential increased. The number of active sites (N_0) on the iodine-modified Au(1 1 1) surface is significantly lower than for copper OPD onto Au(1 1 1). The number of active sites on the iodine-modified Au(1 1 1) surface increased significantly

as the overpotential increased, while the number of active sites for copper OPD onto Au(1 1 1) decreased as the overpotential increased.

4. Conclusions

Under our experimental conditions the measurements showed that the OPD process started before the surface was covered by copper 2D-UPD under iodine. The CV result shows that a highly stable iodine adlayer, that remains in the electrode surface even after copper was several times deposited-striped on/from the gold electrode. The Cu OPD on iodine-modified Au(1 1 1) electrode, under our experimental conditions, was a diffusion-controlled process. The copper OPD nucleation rate (A) on the iodine-modified Au(1 1 1) surface was significantly lower than that of copper OPD onto the bare Au(1 1 1). The copper OPD nucleation rate (A) on the iodine-modified Au(1 1 1) surface increase as the overpotential increased.

Acknowledgements

AMR gratefully thanks O.M. Aguirre (RIP), C. Carballo, M. Miranda Hernandez, J. Valenzuela Benavides, and M.T. Ramirez-Silva for their valuable technical assistance. This work was partially supported by CONACyT through projects grants 24658 and 34132-E and by DCBI-UAMA through projects 2260220 and 2260235. We are indebted to Dr. Mario A. Romero-Romo for fruitful discussion regarding this work and help us with the English translation.

References

[1] R.J. Nichols, D.M. Kolb, R.J. Behm, J. Electroanal. Chem. Interf. Electrochem. 313 (1) (1991) 109.
[2] R. Ullman, T. Will, D.M. Kolb, B. Bunsen-Ges, Phys. Chem. 99 (1995) 1414.
[3] O.M. Magnusen, J. Hotlos, R.J. Nichols, D.M. Kolb, R.J. Behm, Phys. Rev. Lett. 64 (1990) 2929.
[4] O.M. Magnusen, J. Hotlos, R.J. Nichols, D.M. Kolb, R.J. Behm, Vac. Sci. Technol. B 9 (1991) 969.
[5] N. Ikemiya, S. Miyaoka, S. Hara, Surf. Sci. 311 (1994) L641.
[6] M.H. Hölzle, U. Retter, D.M. Kolb, J. Electroanal. Chem. 371 (1994) 101.
[7] M. Palomar-Pardavé, M. Miranda-Hernéndez, I. González, N. Batina, Surf. Sci. 399 (1998) 80.
[8] M. Palomar-Pardavé, I. González, N. Batina, J. Phys. Chem. B 104 (2000) 3545.
[9] A. Martínez-Ruiz, J. Valenzuela-Benavides, L. Morales de la Garza, N. Batina, Surf. Sci. 476 (2001) 139.
[10] A. Martínez-Ruiz, M. Palomar-Pardavé, J. Valenzuela-Benavides, M.H. Farias, N. Batina, J. Phys. Chem. 107 (2003) 11660.
[11] M.H. Hölzle, V. Zwing, D.M. Kolb, J. Electrochim. Acta 40 (1995) 1237.
[12] M.H. Hölzle, C.W. Apsel, T. Will, D.M. Kolb, J. Electrochem. Soc. 142 (1995) 3741.
[13] N.J. Tao, S.M. Lindsay, J. Phys. Chem. 96 (1992) 5213.
[14] T. Yamada, N. Batina, K. Itaya, Surf. Sci. 335 (1995) 204.
[15] N. Batina, T. Yamda, K. Itaya, Langmuir 11 (1995) 4568.
[16] L.H. Mendoza-Huizar, J. Robles, M. Palomar-Pardavé, J. Electroanal. Chem. 521 (2002) 95.
[17] L.H. Mendoza-Huizar, J. Robles, M. Palomar-Pardavé, J. Electroanal. Chem. 545 (2003) 39.
[18] B.R. Scharifker, J. Mostany, M. Palomar-Pardavé, I. González, J. Electrochem. Soc. 14 (1999) 1011.
[19] C. Ramírez, E.M. Arce, M. Romero-Romo, M. Palomar-Pardavé, Solid State Ionics 169 (2004) 81.
[20] J.A. Cobos-Murcia, L. Galicia, A. Rojas-Hernandez, M.T. Ramirez-Silva, R. Alvarez-Bustamante, M. Romero-Romo, G. Rosquete-Pina, M. Palomar-Pardavé, Polymer 46 (2005) 9053.
[21] M. Palomar-Pardavé, B.R. Scharifker, E.M. Arce, M. Romero-Romo, Electrochim. Acta 50 (2005) 4736.
[22] A. Bewick, M. Fleischmann, H.R. Thirsk, Faraday Soc. 58 (1962) 2200.